

CAPACITIVE ARRAYS FOR ROBOTIC SENSING

M. Gimple and B.A. Auld

Edward L. Ginzton Laboratory
Stanford University
Stanford, CA. 94305

INTRODUCTION

Electromagnetic arrays have been used effectively for many years in optimizing the responses of antenna systems. The basic principles that make arrayed antennas work and make them easy to control can also be applied to near field electromagnetic array sensors. The array factor allows for flexibility in sensor geometry. Firstly, by exciting only a portion of an array in a sequential fashion one can physically scan and interrogate a region of a sample without having to move the sample or the probe head itself. Secondly, the field configurations can be altered by selectively exciting electrodes of an array. Also, the information received can be selected by combining electrodes to form different effective receiver geometries. Thirdly, array configurations allow for real-time analog signal processing. For instance, one can perform pattern matching by choosing the spatial resolution of the probe to match the spatial resolution of the desired feature.

The electromagnetic basis of the sensor allows for multi-parameter sensing. First, one can measure distance of the probe from an object by measuring probe electromagnetic coupling with the sample object. Second, the existence and size of flaws can be determined by measuring changes in voltage versus current characteristics at the probe terminals. Thirdly, simple surface features such as edges can be located by using differentially connected probe pairs. Finally, material properties such as dielectric constant and conductivity can be extracted by measuring changes in capacitances and resistances in known geometry samples.

Electromagnetic sensor arrays come in two versions: capacitive and inductive. Capacitive probes are the focus of this paper. Inductive probes are discussed in a companion paper [1] by researchers at SRI.

SAMPLE MATERIALS

Capacitive probes can be used to investigate the properties and structure of both metals and dielectrics. For metals only surface features can be extracted. Charges which accumulate at the surface blind the capacitive probe to interior structures. Dielectrics fortunately do not have this problem. Both surface and interior features can be examined.

PROBE CAPABILITIES

Reference [2] discusses different capacitor array configurations and the capabilities that one can get from such sensing systems. In this paper we demonstrate four such basic capabilities with slight modification:

Distance Ranging
Edge Detection
Response Optimization (Field Adaptation)
Pattern Matching (Filtering)

BASIC PROBE ELEMENT

The basic probe element is shown in Fig. 1(a). It is essentially a parallel plate capacitor that has been opened up such that the two plates lie in the same plane against a common substrate. The electric field lines rather than being parallel (uniform) are now elliptical (non-uniform). The probe is operated by applying a voltage to one electrode and measuring the current to ground from the second electrode (receiver). Interrogated samples are placed in the lower half space. Changes in measured current reflect changes in the sample-probe system configuration. A metal sample, which is grounded, when placed close to the electrodes will shunt current around the receiver electrode to ground and thus lower the output signal. Dielectrics on the other hand will enhance the output for they increase the capacitive coupling between the sensing electrodes, without shunting any significant current to ground.

For a single port eddy current device we know [3] that the change in impedance is given by

$$\Delta Z = \frac{j\omega\mu_0}{I^2} \int \left(\left\{ \frac{\partial}{\partial z} \phi \right\} \phi' - \phi \left\{ \frac{\partial}{\partial z} \phi' \right\} \right) dx dy \quad (1)$$

where ϕ is the magnetostatic potential ($H = \nabla\phi$) and the integration is performed over the surface of the mouth of the flaw. The primed notation refers to those quantities that exist in the presence of the flaw. The unprimed quantities refer to flaw absence. For the capacitive device described above we have a dual relationship, that is,

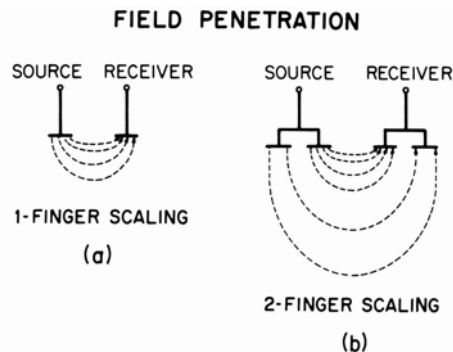


Fig. 1. Elementary capacitive probes. They are used for distance ranging.

$$\Delta y = \frac{j\omega\epsilon_0}{v^2} \int \left(\psi \frac{\partial \psi'}{\partial z} - \psi' \frac{\partial \psi}{\partial z} \right) dx dy \quad (2)$$

ψ is the electrostatic potential ($E = -\nabla\psi$) and the integration is performed over the surface of the test piece. Solutions for simple geometries can be extracted directly. For more complex geometries approximations and numerical techniques must be employed.

Figure 1(b) shows a similar configuration to that in Fig. 1(a) except that the source now consists of two contiguous, elementary electrode fingers excited simultaneously and the receiver consists of two contiguous, elementary electrode fingers whose currents outputs are added together. As shown in the figure this allows for deeper field penetration and higher sensitivity at a given distance away.

Experiments demonstrating this effect were conducted using these probes with metallic samples. The electrodes that were used were 40 mils wide and 475 mils long. They were separated by 50 mils. A full array of electrodes were employed (8 to 9 fingers) even though only a subset was actively involved in the measurements. The remaining electrodes were explicitly grounded. Experimental results are shown in Fig. 2. In order that the two geometries could be compared on a similar basis both outputs were normalized to a 0dB level at the zero vertical distance position. Note that the curve for the two-finger scaled probe dominates over that for the 1-finger scaling case. This is an indication that the fields do penetrate further into the interrogation region when the effective electrode widths are increased. Also note that for extremely small vertical distances the sensitivity of the probes to distance (slope) is small. This is due to the fact that at small distances the metal sample is so close to the source electrodes that it completely shields the receiving electrode from any interaction.

COMPLEX ELECTRODE CONFIGURATIONS

The configurations of Fig. 1 are sensitive to both vertical distances and horizontal displacements. Separating the two effects from each other is not readily done with a two electrode probe. Thus, there

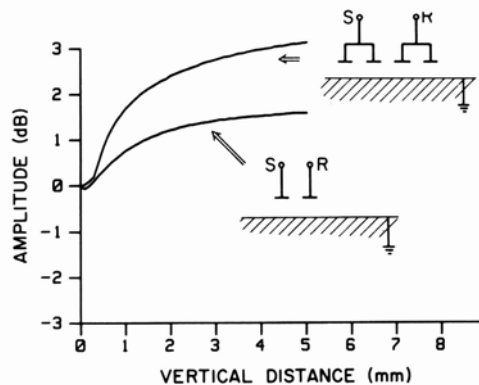


Fig. 2. Normalized distance ranging output for the two elementary capacitive probes.

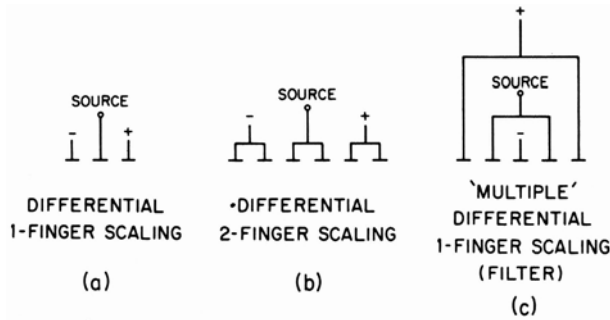


Fig. 3. Three complex electrode probe configurations. They are used to extract lateral surface features.

is a need to adopt a probe geometry having a greater number of source/receiver electrodes. Figure 3 displays electrode configurations that make use of multiple source/receiver electrodes, with differential electronics to eliminate signals from common mode effects. Changes that affect both sides of the differential pair similarly (such as changes in vertical distances) are nulled. Only changes that disturb parts of the probe fields will result in non-zero outputs. Figure 3(a) is the simplest differential configuration. It is essentially two elementary probes connected in tandem with opposite polarity.

Experimental results for a grounded metal, slotted sample are shown in Fig. 4. The slots are .75 inches wide and 10 mils and 5 mils deep, respectively. The sample is scanned in a direction perpendicular to the sample slots. The probe is oriented such that the scan direction is perpendicular to electrode fingers. The peaks and valleys in the signal correspond to the edge components of the slots. A point to note is that the response to the deeper slot is larger than the response to the shallower slot. Thus, the probe is sensitive to slot depths. Also note that the response for a given depth slot is not symmetric for each edge (i.e. the size of the peak does not equal the size of the valley). This is due to the fact that the differential electronics is not balanced to zero. This purposeful asymmetry in gain paths allows us to measure output signal polarity from the signal amplitude alone.

Figure 5 displays results for a dielectric sample. The sample used is Delrin ($\epsilon_r = 3.7$). The three slots are .625 inches wide and 20

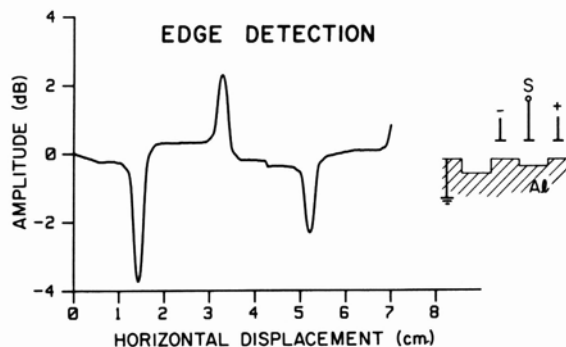


Fig. 4. Horizontal scan of a slotted Al sample with a 1-finger scaled differential probe. The slot depths are 10 mils and 5 mils, respectively. The sample is explicitly grounded.

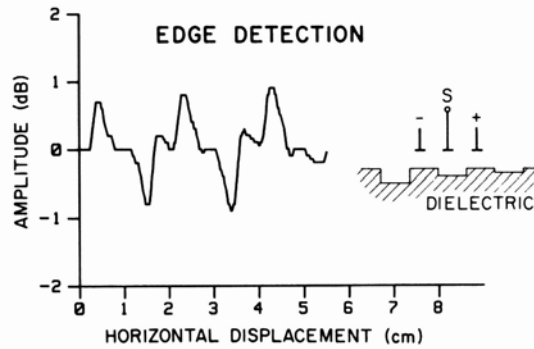


Fig. 5. Horizontal scan of a slotted Delrin sample with a 1-finger scaled differential probe. The slot depths are 20 mils, 10 mils, and 5 mils, respectively.

mils, 10 mils, and 5 mils deep, respectively. Note, that in the dielectric case a peak (valley) in the output signal occurs where a valley (peak) would occur with a metal sample. Also, one should note that the probe's sensitivity to each of the dielectric slots is the same (each peak and valley is of approximately the same size). We infer from this that the probe's sensitivity reaches saturation at a point under 5 mils deep. Further investigation is needed here.

Figure 3(b) displays a configuration similar to Fig. 3(a) save for the fact that 2-finger scaling is employed. One should expect better sensitivity but lower horizontal resolution than in the 1-finger scaling case. The lower horizontal resolution is due to the fact that an edge disturbance starts to cause a mismatch as it starts passing over the receiver electrodes and reaches maximum mismatch when the edge is centered on the source electrode. Since 2-finger scaling probes are physically larger, then the peaks and valleys in the signals will be wider. Experimental results are displayed in Fig. 6.

The third differential probe consists of two single differential probes connected in tandem with the opposite polarity (see Fig. 3(c)). The purpose of this probe configuration is to look at two features (edges) simultaneously that are separated in space (filtering). When

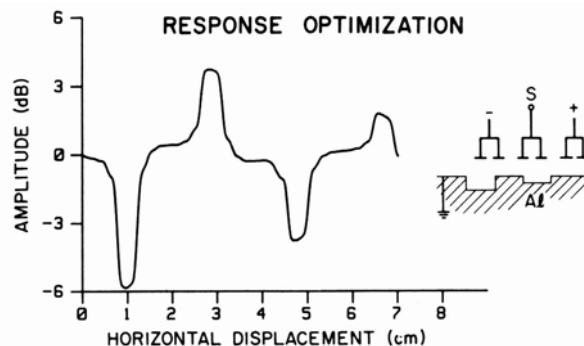


Fig. 6 Horizontal scan of a slotted Al sample with a 2-finger scaled differential probe. The slot depths are 10 mils and 5 mils, respectively. The sample is explicitly grounded.

the spatial separation of the sample edges matches the spatial separation of the source electrodes then the output signal will be the sum of two edge signals overlapping giving a large peak or valley. At any other slot width the output signal tends to separate into two smaller individual signals. The degree of separation is dependent not only on the slot width itself but also on the width of the impulse response of the probe. Figure 7 displays experimental results for this probe scanned over three slots of widths of .180 inches (matched) .125 inches, and .500 inches, respectively in an explicitly grounded metal sample.

To apply capacitive probes to quantitative nondestructive evaluation and intelligent robot sensing it is necessary to quantitatively interpret the probe signals. This requires the development of probe interaction modeling based on Eq. (2). In investigating the behavior of long arrays, one can first approximate the probe as though it is of infinite extent. For an infinite array the analytical solution for the electric fields in the interrogating half-space without any samples present is given by [4]. The solutions are in the form of summations of Legendre polynomials. We are investigating the area of using perturbation methodologies to extract the field expressions that occur when sample objects are present with and without surface features such as edges and slots. This is an area of future work, and will be extended using finite difference calculations for the various probe geometries discussed above.

CONCLUSION

Four basic capabilities of capacitive arrays have been demonstrated. Also it has been demonstrated that capacitave arrays can be effective for both metals and dielectrics.

Future plans involve developing more analytical modeling capacity in order to produce better probes and to eliminate the need for recalibration for new sample geometries. Considerations for future probes include extending array geometries into 2-D and incorporating microelectronic preamplification in close proximity to the measuring electrodes.

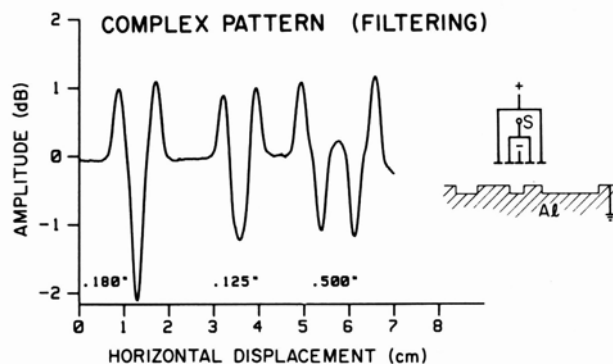


Fig. 7 Horizontal scan of a slotted Al sample with a spatial filter probe. The slots are 20 mils deep and are .180 inch (matched), .125 inch, and .500 inch wide, respectively. The sample is explicitly grounded.

ACKNOWLEDGEMENTS

We would like to thank A.J. Bahr and A. Rosengreen at SRI for their close collaboration. The work done here has been sponsored by the Air Force under Contract No. F49620-84-C-0095.

REFERENCES

1. A. J. Bahr and A. Rosengreen, in: these proceedings.
2. B. A. Auld, J. Kenney, and T. Lookabaugh, "Electromagnetic Sensor Arrays-Theoretical Studies", in: Review of Progress in Quantitative Nondestructive Evaluation 5A, D. O. Thompson and D. E. Chimenti, eds., (Plenum Press, New York, 1985).
3. B. A. Auld and S. Jefferies; J. C. Moulder and J. C. Gerlitz, "Semi-Elliptical Surface Flaw EC Interaction and Inversion Theory", in: Review of Progress in Quantitative Nondestructive Evaluation 5A, D. O. Thompson and D. E. Chimenti, eds., (Plenum Press, New York, 1985).
4. D. P. Morgan, "Surface-Wave Devices for Signal Processing", (Elsevier Science Publishers, Amsterdam, 1985) 335-361.